Nanoscale

Accepted Manuscript

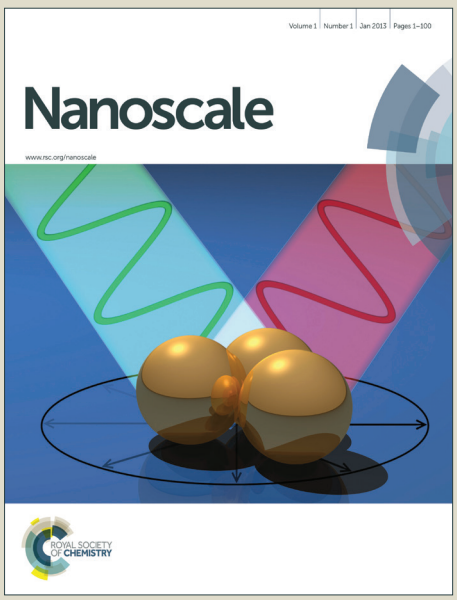

ROYAL SOCIETY OF CHEMISTRY

www.rsc.org/nanoscale

Nanoscale

RSCPublishing

ARTICLE

Strong slip-induced anomalous enhancement and red-shifts in wide-range optical absorption of graphite under uniaxial pressure

Cite this: DOI: 10.1039/x0xx00000x

Received ooth January 2012,
Accepted ooth January 2012

DOI: 10.1039/x0xx00000x

www.rsc.org/

Ji-Chang Ren,[abc] Rui-Qin Zhang,[*a] Zejun Ding[*b] and Michel A. Van Hove[*d]

Natural graphite shows little optical response. Based on first-principles calculations, we demonstrate, for the first time, that in-plane pressure-induced slip between atomic layers causes a strong anomalous enhancement and large red-shifts in the infrared and far infrared optical absorption by graphite. Specifically, slip along the armchair direction induces an absorption feature that redshifts from ~3 eV to ~0.15 eV, while its intensity increases by an order of magnitude, due to an electron density delocalization effect with slip. Our results provide a way to detect and measure the magnitude of the in-plane slip of graphite under compression and also open up potential applications in electronics and photonics.

Introduction

In nature, most graphite phases exist in the AB-stacking arrangement[1-5] with weak interlayer interactions, whereas in compressed graphite the interplay of adjacent layers could become much stronger. Recently, a new phase of super-hard graphite has been observed experimentally[6], followed by theoretical workwhich proposed possible structures of this metastable state[7-13]. It is shown that most of these proposed structures are consistent with the experimental data[9-13]. However, it is difficult to elucidate which of these candidates exist or coexist in the super-hard phase, making the transformation of this phasemore mysterious.

In contrast to hydrostatic pressure, little computational work has been carried out for graphite under uniaxial pressure[14], which is important for the following reasons. Firstly, under uniaxial pressure, graphite prefers to orient its *c* axis parallel to the direction of pressure[6]. Secondly, the interaction between graphite-diamond transformation. Molecular dynamics studies have found that in-plane relative shifts of adjacent graphene layers occur before transformation to diamond[15] and this was explained by a concerted mechanism[16].

Recently, a nucleation mechanism was proposed to describe the graphite-diamond transformation, which is closer to observations[17]. Both of the mechanisms hypothesize the slipping of graphene layers before the buckling of the layers. To the best of our knowledge, no measurable parameter has been reported that exposes or quantifies the slip of graphene layers; and it is necessary to theoretically evaluate the slip character of graphite under compression to better understand graphite-diamond transformation. In addition, under compression, large hybridization of interlayer π/π^* orbitals, contrasting with little modification of σ orbitals, induces changes in optical reflectivity[18]. Also, for graphite related materials, the optical responses are largely related to their different stacking arrangements[19-21]. Therefore, understanding the slip behavior of graphite and its corresponding optical absorption under high uniaxial pressure is of great importance in graphite-diamond transformation and its potential application in electronics and photonics.

This paper theoretically predicts a strong new effect which can now be measured experimentally. In this study, we simulated the uniaxial compression perpendicular to the

[a]*Department of Physics and Materials Science, City University of Hong Kong, Hong Kong SAR, China. E-mail: aprqz@cityu.edu.hk;*
[b]*Department of Physics, University of Science and Technology of China,Hefei, China. E-mail: zjding@ustc.edu.cn*
[c]*USTC-CityU Joint Advanced Research Centre, Suzhou, 215123, China*
[d]*Institute of Computational and Theoretical Studies & Department of Physics, Hong Kong Baptist University, Hong Kong SAR, China. E-mail:vanhove@hkbu.edu.hk*

graphite plane. By calculating the interlayer interaction energy, we find that spontaneous in-plane slip occurs under high compression and that under ultrahigh pressure the slip barrier decreases with increasing applied pressure. The in-plane slip induces a strong enhancement and large red-shifts of a broad optical absorption peak that spans from the ultraviolet to the far infrared region. Our detailed study shows that the absorption energies of the feature are nearly totally dependent on the relative positions of interlayer carbons. Thus, our finding provides a possible measurable parameter to detect the slip of graphite layers before graphite-diamond transformation occurs. The slip-dependent optical absorption can act as a detector of in-plane slip of graphite under high pressure.

As reflected in the large interlayer distance of graphite, the interaction between adjacent layers is dominated by van der Waals forces. The weak coupling induces two inter-band transition thresholds at about the *K* point near the Brillouin-zone edge[22], resulting in near-infrared optical absorption. A study of the band structure of graphite under uniaxial pressure parallel to the *c* axis showed[14] that the band dispersion around the symmetric *K* point is very sensitive to the applied pressure. However, the previous studies have not revealed the slip of graphene layers because relatively small applied pressures were used. Thus, the fact that optical absorption responds to the slip of graphene layers is also a fundamentally important topic.

Computational details

In this paper, the slip barrier of graphite and optical absorption calculations under uniaxial pressure were carried out using the Density Functional Theory (DFT) based SIESTA package[23]. A series of uniaxial pressures parallel to the *c* axis ranging from 0 GPa to 120 GPa were applied to AB-stacked graphite. The GGA scheme of PBE type[24] was used and the Norm Conserving pseudopotential[25] was selected to describe carbon. An energy cutoff (for a real space mesh size) of 400 Ry was used and a double-ζ plus polarization basis set was applied for the localized basis orbitals. The cut-off radius is 4.63 Bohr for the 2*s* orbital of carbon atom and 5.66 Bohr for the 2*p* orbital of carbon atom, which was performed by setting an energy-shift of 100 meV. For the geometric relaxation, the cell lattices were all allowed to relax freely during the structure optimization and the convergence was assumed to be reached when the forces on each atom were less than 0.005eV/Å. The dielectric function calculations were carried out by first-order time-dependent perturbation theory[26]. The theory treats the external perturbation as a time-dependent value, and by calculating the dipolar transition matrix between occupied eigenstates and unoccupied eigenstates with single-electron description, we obtained the approximated dielectric function[23] (a discussion of the method can be found in Supplemental Material). The polarization of the electric field vector was set along the *c* axis for the optical absorption calculations. The imaginary part of the dielectric function, which corresponds to the absorption spectra, was studied. The three-dimensional Brillouin zone integration was sampled by 6×6×6 k-points for structural optimization and 60×60×60 k-points for electronic structure and optical absorption calculations.

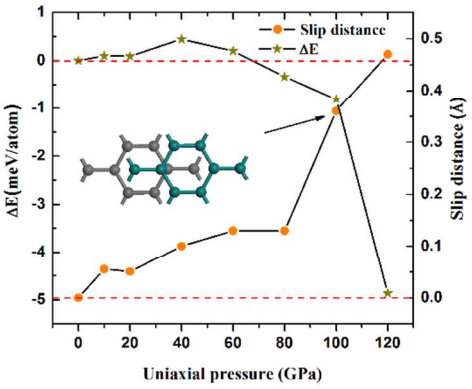

Fig.1 The energy difference ΔE and the slip distance as a function of uniaxial pressure. Here $\Delta E = (E_{opt-slip} - E_{no-slip})/N$, where $E_{no-slip}$ is the total energy of thecompressed system with an AB-stacking arrangement, $E_{opt-slip}$ the total energy of the compressed slip system obtained by structure optimization under compression, and N the number of carbon atoms in the system. The dashed lines emphasize the values for the uncompressed system, for reference.

Results and discussion

Through geometric relaxation, we find that the compression can induce slip perpendicular to the pressure direction, as shown in Fig. 2(a), even though, because of symmetry, this slip direction is not obvious; one way to rationalize such a slip is that pairs of atoms with mutual A-A or B-B "on-top" alignment in adjacent layers can be forced to roll sideways under pressure, thus breaking the bulk's normal 3-fold rotational symmetry.

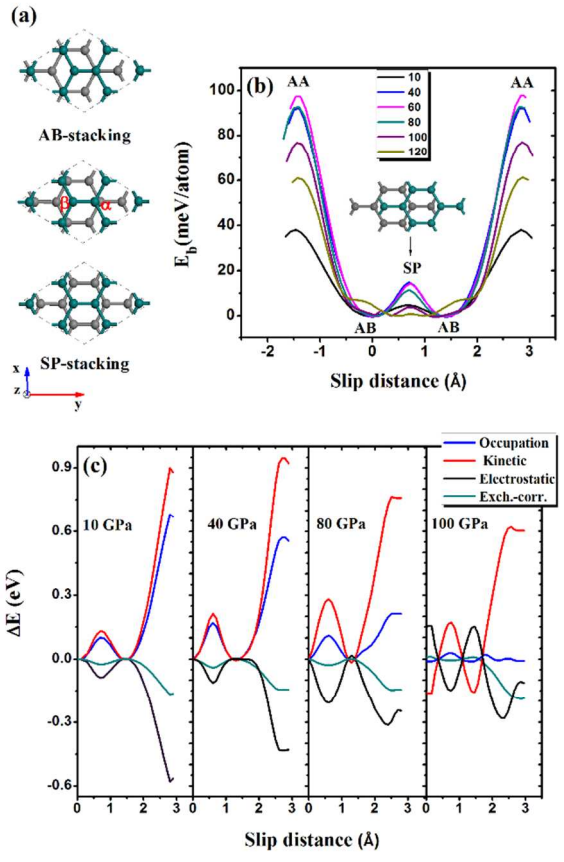

Fig.2 (a) Schematic of AB-stacked graphite under uniaxial pressure. The *z* axis is also the crystallographic *c* direction. The *y* axis is along the armchair direction. Applied uniaxial pressure along *c* induces a

relative slip of graphene layers along the armchair direction y (or equivalent symmetrical directions). (b) The interlayer interaction energy E_b as a function of slip distance under different uniaxial pressures. The inset shows SP stacking viewed perpendicularly to the atomic layers; the high barriers correspond to AA-stacking. $E_b = (E_{opt-slip} - E_{slip})/N$, where E_{slip} is the total energy of the system with different slip distances, $E_{opt-slip}$ the total energy of the compressed slip system obtained by structure optimization under compression, and N the number of carbon atoms in the system.And (c) the decomposition of the total energy into Occupation energy, Kinetic energy, Electrostatic energy and Exchange-correlation (Exch.-corr.) energy, as a function of slip distance. The ground state energies are set to zero.

The comparison of total energies between compressed slip systems and the compressed no-slip systems with AB-stacking arrangement (in Fig. 1) shows that a relative slip of graphene layers is favored at high uniaxial pressure. It has been reported, based on constant-pressure *ab initio* molecular dynamics calculations[15], that the slip of graphene layers occurs before collapse and buckling of the graphene layers and that the compressed graphite alternatively changes into hexagonal and orthorhombic structures under different pressures at a constant temperature. This indicates that a barrier may exist for the system to reach the orthorhombic structures when the applied pressure is not large enough. The question arises: How difficult is it to make the graphene layers slip under compression?

To reveal the slip barrier of graphite under compression, we calculated the interlayer interaction energy E_b as a function of the interlayer slip along the armchair direction. It shows that, when the uniaxial pressure is larger than 60 GPa, the slip barrier at SP (Fig. 2(b)) decreases with increasing compression. In the meantime, the AB-stacking system shows an increased energy barrier. It indicates that graphite prefers a nearly SP-stacked arrangement under high compression.

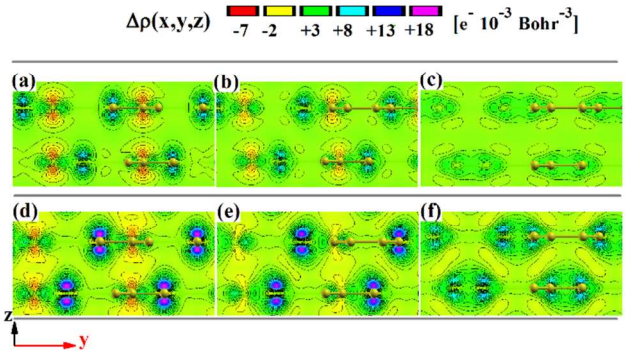

Fig. 3 Differential charge distribution $\Delta\rho$ in the y-z plane, where y is along the armchair direction, and z along the c-axis of the system, so the graphite layers are seen edge-on horizontally: (a)-(c) ((d)-(f)) show the systems under 40 GPa (100 GPa) with slip distances 0.0 Å, 0.36 Å, and 0.70 Å, respectively, along the armchair direction. $\Delta\rho = \rho_{12} - \rho_1 - \rho_2$, where $\Delta\rho$ is the charge density of the compressed graphite, while ρ_1 and ρ_2 are the charge densities of systems obtained by removing all A or all B graphene layers respectively, so as to minimize interlayer interactions.

Interestingly, the corrugation of E_b firstly increases then decreases with rising uniaxial pressure, which behavior deviates from Amonton's Law of Friction. In order to provide insight into this anomalous behavior, we decomposed the total energy into four parts, as indicated in Fig. 2(c). For the systems with slip, kinetic energy is almost offset by electrostatic energy, giving no contribution to the slip barrier, except for the slip close to AA-stacking. In Fig. 2(c), it can be seen that the occupation energy dominates the slip barrier in the AB-SP-AB region, which indicates that the changes of occupation states are due mainly to the slip barrier. A further look at the charge density difference (Fig. 3) shows that the slip barrier is influenced by localization of the electron density, which can be explained as follows. Compression inevitably induces overlap of the charge distributions. Simultaneously, Pauli repulsion forces the electrons to transfer from "on-top" carbon atoms to "hollow" carbon atoms. Slip delocalizes the electrons when slipping towards SP-stacking. Due to delocalization, on one hand, the screening effect is enhanced, and consequently, the electrostatic energy is reduced; on the other hand, the delocalization increases the Pauli repulsion induced by the overlapping electron distributions from nearby carbon atoms, which corresponds to the increase of occupation energy in Fig. 2(c). Since the contribution made by the screening effect is almost cancelled by the kinetic energy, the slip barrier at SP is mainly caused by the changes of the occupation, which relates to the delocalization effect induced by slip. When the pressure is larger than 60 GPa, the delocalization effect is reduced with slip. Therefore, the slip barrier decreases with increasing pressure.

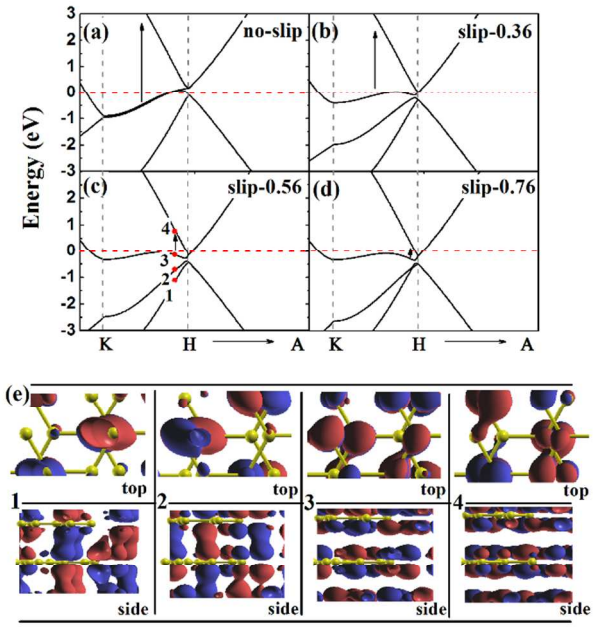

Fig. 4 (a)-(d) Band structure (along *M*-*K*-*H*-*A*) of graphite under 100 GPa with slip distances of 0.0 Å, 0.36 Å, 0.56 Å and 0.76 Å, respectively. The arrows indicate the electron transitions of the systems. (e) Wave-functions of the compressed graphite with slip distance 0.56 Å (as in panel *c*), in top and side views (upper and lower panels) relative to the atomic planes. 1 (*α*-*n*-*n* bonding state), 2 (*β*-*n*-*n*bonding state), 3 (*β*-*n*-*n*anti-bonding state), and 4 (*α*-*n*-*n* anti-bonding state) correspond to the particular k-points denoted in (c).

As a result, the stacking arrangement departs from AB-stacking, which reduces the symmetry of the system. Consequently, the optical absorption may also be influenced.

Thus, it may be possible to determine the slip behavior by measuring the changes of optical absorption, as we examine next.

The absorption character is determined by the unique band structures of this material. From the viewpoint of the geometric structure, there are mainly two changes: interlayer distance and relative position of carbon atoms in the adjacent layers. Thus, we calculated the band structures of compressed graphite with AB-stacking and those with slip but with the interlayer distance maintained constant.

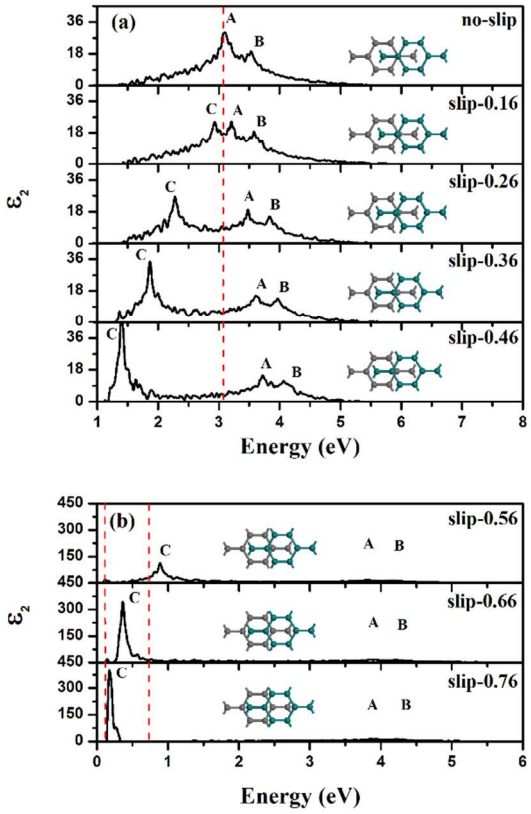

Fig. 5 (a) and (b) Imaginary part of the dielectric function of graphite under 100 GPa for a series of slip distances from AB-stacking to SP-stacking (0.0 Å, 0.16 Å, 0.26 Å, 0.36 Å, 0.46 Å, 0.56 Å, 0.66 Å, and 0.76 Å). The insets show the respective slip structures. The axis scales are changed between (a) and (b) for clarity.

For the band structure of graphite without slip under uniaxial pressure, an evident change occurs along the *K*—*H* direction in the Brillouin zone (Fig. 4(a)). For natural graphite, one degenerate flat band is located right at the Fermi level with two nearby bands above and below. These two bands are related to π and π* orbitals, respectively. After uniaxial pressure is applied, the lower band shifts down and the upper band shifts up, which indicates stronger interlayer coupling compared with natural graphite (see Supplemental Material). Due to strong Pauli repulsion between "on-top" carbon atoms, the in-plane π orbitals are partly destroyed, as is seen in Fig. 3(a)-(f). Consequently, both bands change: the occupied one is the coupling of the non-bonding orbital *n* of "on-top" (A-A or B-B aligned) carbon atoms, which can be defined as *n*-*n* bonding state, while the unoccupied one is *n*-*n* anti-bonding state. Naturally, the π electron orbital in graphite shows very high rigidity,[27] which excludes interlayer bonding state. However, with the interlayer distance decreased due to the increased Pauli repulsion, the rigidity of π electronic structure gradually reduces. Consequently, the interlayer electronic coupling is enhanced. It is noted that the unoccupied bands along the *K*—*H* direction bend down across the Fermi level and form an "electron pocket" at higher pressure (see Supplemental Material). This indicates enhancement of the conductivity perpendicular to the graphene layers. In addition, with the increase of uniaxial pressure (⩾ 40GPa), the energy bands similar to Dirac cone appear around the H point, indicating that Dirac fermions exist at the interface between neighboring layers.

In contrast to the no-slip systems, the slip effect mainly modifies the bent degenerate band across the Fermi level along the *K*—*H* direction. In Fig. 4(b-d), the degenerate band splits into two separate bands with slip towards SP-stacking. The lifting of degeneracy is induced by the reduction of symmetry of the slip systems. As the systems slip along the armchair direction, the previous "on-top" carbons depart from each other, while the previous "hollow" carbons move closer together; only for SP-stacking do all the carbons feel the same surroundings. We denote the previous "on-top" carbon as α-carbon and previous "hollow" carbon as β-carbon, as shown in Fig. 2(a). The previous interlayer *n*-*n* bonding state and *n*-*n* anti-bonding state are split into *α*-*n*-*n*, *β*-*n*-*n* bonding states and *α*-*n*-*n*, *β*-*n*-*n* anti-bonding states respectively (Fig. 4(e)). With the system sliding towards SP-stacking, the surroundings of α-carbon atoms and β-carbon atoms tend to become identical. Thus, the energy difference between α-*n*-*n* and β-*n*-*n* orbitals is reduced.

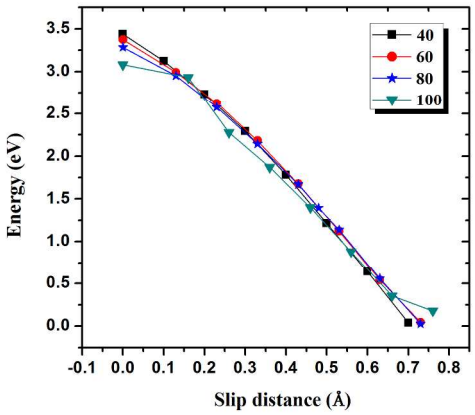

Fig. 6 The absorption position of the peak C shows redshifts as a function of slip distance at uniaxial pressures 40, 60, 80 and 100 GPa, as identified in the inset.

To evaluate the optical response of the compressed graphite with slip, we calculated the imaginary part of the dielectric function of the slip systems under a polarized electric field perpendicular to the graphene layers. Fig. 5 shows the imaginary part of the dielectric function of graphite for an interlayer slip along the armchair direction, under 100 GPa uniaxial pressure. Two peaks appear for the system without slip, denoted A and B. As has been noted[14], they are induced by π to π* transitions near the L point of the Brillouin zone. They show slight blue-shifts with increasing slip. A strong new absorption peak appears at lower energy when introducing slip to the compressed system, denoted C in Fig. 5. It is observed that absorption peak C is very sensitive to the relative slip of

graphene layers. It shows strong redshifts and a large enhancement of absorption in the slip process from AB-stacking to SP-stacking. The shift of this feature spans from the ultraviolet to the infrared parts of the spectrum.

The absorption feature C emerges once the stacking arrangement deviates from AB-stacking and the symmetry of the system is reduced. As seen in Fig. 5, peak C shifts from 2.92 eV to 2.28 eV when the slip distance changes from 0.16 Å to 0.26 Å. Such large energy shifts can easily be detected experimentally. In addition, the intensity of the absorption is strongly enhanced, by an order of magnitude, when graphite slips towards the SP-stacking arrangement. By analyzing the band structures and the wave-functions of the slip systems, we find that the peak C is derived from the transition from the anti-β-*n*-*n* orbital to the anti-α-*n*-*n* orbital. Due to the change of symmetry, the transition moves towards the H point with increasing pressure. Thus, large redshifts of peak C occur for the compressed systems sliding toward SP-stacking.

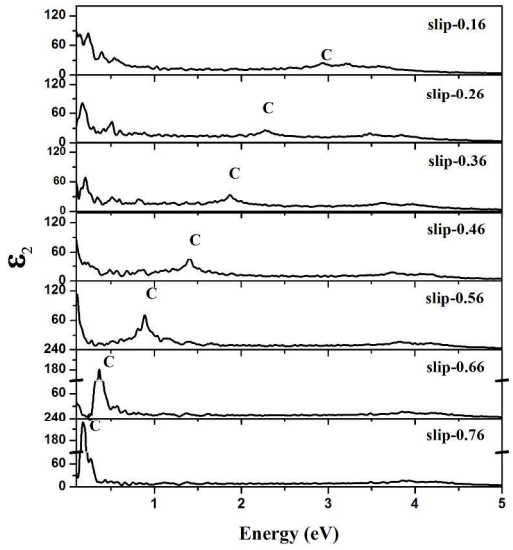

Fig. 7 Imaginary part of the dielectric function of polycrystalline graphite under 100 GPa for a series of slip distances from the AB-stacking to the SP-stacking (the labels indicate slip distances of 0.16 Å, 0.26 Å, 0.36 Å, 0.46 Å, 0.56 Å, 0.66 Å, and 0.76 Å).

It should be noted that the absorption is tremendously enhanced in the infrared region when the system approaches SP-stacking. As is shown in Fig. 5(b), at slip distance 0.56 Å, the absorption peak is located at ~0.9 eV, while when the slip approaches SP-stacking, e.g., at 0.76 Å, the absorption peak shifts down to ~ 0.15 eV. Comparing Fig. 5(a) and (b), we thus conclude that the absorption intensity increases anomalously when sliding towards SP-stacking. It has been reported experimentally that natural graphite shows universal optical conductance in the energy region 0.1 - 0.6 eV[28]. Recently, a study of bilayer graphene nanoribbons has revealed a strong optical response in the THz and far infrared regime due to the interaction of the ribbons' chirality and the inter-ribbon coupling[29]. In this study, we propose that the absorption spectra can be significantly enhanced in the energy range from 0.12 to 1.0 eV by sliding graphite close to the SP stacking under high uniaxial pressure. The abnormal enhancement of absorption intensity can be attributed to the symmetry breaking induced by the slip, which causes the relaxation of selection rules. In addition, the application of uniaxial pressure causes the accumulation of charge around graphene layers (see Supplemental Material). The gathered electrons mainly occupy π/π^* and *n* orbitals, which significantly enhances the absorption intensity.

For comparison with the effect of in-plane slip, we have calculated the redshifts of slip systems with different interlayer distances, as shown in Fig. 6. We find that the redshifts of the C peak show a similar trend with slip under different compression. This indicates that the relationship between redshifts of the peak C and interlayer slip is almost independent of the interlayer distance. Thus a robust signal is available to detect the slip of graphite. A further calculation shows that even for polycrystalline graphite (in Fig. 7) the in-plane slip can also induce significant redshifts and strong anomalous enhancement of peak C when the slip system is close to SP stacking. Due to the strongly anisotropic character of graphite, the absorption features along other directions can hardly merge into peak C. Thus, the redshifts of the enhanced spectrum provide a way to detect and measure the graphite in-plane slip resulting from uniaxial pressure.

Conclusions

In conclusion, the slip of graphite along the armchair direction under uniaxial pressure involves a slip barrier which initially increases with pressure. However, when the pressure exceeds about 60 GPa, the slip barrier decreases markedly. This abnormal behavior is mostly attributed to the decline of the delocalization effect with slip. The optical response to the slip of graphite under compression is very sensitive to the in-plane slip of graphene layers. When graphene layers slip from AB-stacking to SP-stacking, a new absorption feature shows strong redshifts and a large enhancement which spans from the ultraviolet to the far infrared region. An unexpected enhancement of the absorption peak by an order of magnitude appears in the far-infrared region when the stacking arrangement approaches SP-stacking. This feature is due to the symmetry breaking by the slip. The observed redshifts of the new peak are caused by transition from anti-β-*n*-*n* orbitals to anti-α-*n*-*n* orbitals. Our finding offers a method to detect and quantify the in-plane slip of graphite under pressure. In addition, the tunable optical absorption in the low energy range may be explored for application in electronics and photonics.

Acknowledgements

The work described in this paper was supported by a grant from the Research Grants Council of the Hong Kong Special Administrative Region (HKSAR) [project No. CityU 103812], and Centre for Functional Photonics (CFP). MAVH was supported by the HKBU Strategic Development Fund. We thank the High Performance Cluster Computing Centre, Hong Kong Baptist University, which receives funding from the Research Grants Council, University Grants Committee of the HKSAR and Hong Kong Baptist University.

Notes and references

Electronic Supplementary Information (ESI) available: [details of any supplementary information available should be included here]. See DOI: 10.1039/b000000x/

1 Z. Y. Rong and P. Kuiper, *Phys. Rev. B*, 1993, **48**, 17427–1743.
2 J. W. McClure, *Carbon*, 1969, **7**, 425-522.
3 J. C. Charlier, X. Gonze, and J. P. Michenaud, *Carbon*, 1994, **32**, 289-299.
4 P. J. Ouseph, *Phys. Rev. B*, 1996, **53**, 9610.
5 J. C. Charlier, J. P. Michenaud, and X. Gonze, *Phys. Rev. B*, 1992, **46**, 4531.
6 W. L. Mao, H.-K. Mao, P. J. Eng, T. P. Trainor, M. Newville, C.-C. Kao, D. L. Heinz, J. Shu, Y. Meng, and R. J. Hemley, *Science*, 2003, **302**, 425.
7 C. He, L. Sun, C. Zhang, X. Peng, K. Zhang, and J. Zhong, *Phys. Chem. Chem. Phys.*, 2012, **14**, 8410.
8 D. Selli, I. A. Baburin, R. Martoňák, and S. Leoni, *Phys. Rev. B*, 2011, **84**, 161411(R).
9 Q. Li, Y. Ma, A. R. Oganov, H. Wang, H. Wang, Y. Xu, T. Cui, H. K. Mao, and G. Zou, *Phys. Rev.* Lett., 2009, **102**, 175506.
10 M. Amsler, J. A. Flores-Livas, L. Lehtovaara, F. Balima, S. A. Ghasemi, S. Botti, A. San Miguel, S. Goedecker, and M. A. L. Marques, *Phys. Rev. Lett.*, 2012 **108**, 065501.
11 K. Umemoto, R. M. Wentzcovitch, S. Saito, and T. Miyake, *Phys. Rev. Lett.*, 2010, **104**, 125504.
12 J.-T. Wang, C. Chen, and Y. Kawazoe, *Phys. Rev. Lett.*, 2011, **106**, 075501.
13 D. Selli, I. Baburin, R. Martoňák, and S. Leoni, *Phys. Rev. B*, 2011, **84**, 161411.
14 R. Ahuja, S. Auluck, T. J., J. M. Wills, O. Eriksson, and B. Johansson, *Phys. Rev. B*, 1995, **51**, 4813.
15 S. Scandolo, M. Bernasconi, G. L. Chiarotti, P. Focher, and E. Tosatti, *Phys. Rev. Lett.*, 1995, **74**, 4015.
16 Y. Tateyama, T. Ogitsu, K. Kusakabe, and S. Tsuneyuki, *Phys. Rev. B*, 1996, **54**, 14994.
17 R. Z. Khaliullin, H. Eshet, T. D. Kühne, B. J., and M. Parrinello, *Nature Mater.*, 2011, **10**, 693.
18 M. Hanfland and K. Syassen, *Phys. Rev. B*, 1989, **40**, 1951.
19 Y. Qian, K. Lam, C. Lee, and G. Liang, *Carbon*, 2012, **50**, 1659.
20 M. Koshino, *New Journal of Physics*, 2013, **15**, 015010.
21 I. Lin, J. Liu, K. Shi, P. Tseng, K. Wu, C. Luo, and L. Li, *Phys. Rev. B*, 2012, **86**, 235446.
22 G. Guizzetti, L. Nosenzo, E. Reguzzoni, and G. Samoggia, *Phys. Rev. Lett.*, 1973, **31**, 154.
23 J. M. Soler, , E. Artacho, J. D. Gale, A. Garcia, J. Junquera, P. Ordejon, and D. Sánchez-Portal, *J. Phys. Condens. Matter*, 2002, **14**, 2745.
24 J. P. Perdew, K. Burke, and M. Ernzerhof, *Phys. Rev. Lett*., 1996, 77, 386.
25 N. Troullier and J. L. Martins, *Phys. Rev. B*, 1991, 43, 1993.
26 E. N. Economou, Green's Functions in Quantum Physics (Berlin: Springer), (1983).
27 C.S. Guo, W.J. Fan, and R.Q. Zhang, *Appl. Phys. Lett.*, 2009, **89**, 123103.
28 A. B. Kuzmenko, E. van Heumen, F. Carbone, and D. van der Marel, *Phys. Rev. Lett.*, 2008, **100**, 117401.
29 A. R. Wright, J. C. Cao, and C. Zhang, *Phys. Rev. Lett.*, 2009 **103**, 207401.

